Acicular iron nanoparticles protected against sintering with aluminium oxide

R. POZAS[1], M. P. MORALES[2], C. J. SERNA[2], M. OCAÑA[1]

[1] Instituto de Ciencia de Materiales de Sevilla (CSIC-UNSE), Américo Vespucio s/n, Isla de la Cartuja, 41092 Sevilla, Spain.
[2] Instituto de Ciencia de Materiales de Madrid (CSIC), Cantoblanco, 28049 Madrid, Spain.

Acicular iron nanoparticles have been obtained by thermal reduction with hydrogen of a goethite precursor protected against sintering with Al cations, either by doping during the synthesis or by a further coating and the relation between microstructure and magnetic properties of the final Fe particles has been studied in order to evaluate the efficiency of both protecting methods. Uniform goethite and Al-doped goethite precursors were prepared by oxidation with air of $FeSO_4$ solutions, containing $Al(NO_3)_3$ when required, previously precipitated with Na_2CO_3, while the Al oxide coating on the undoped goethite precursor was carried out by heterocoagulation. In both protecting methods, Al cations were mainly concentrated in the particle outer layers of the goethite precursors and the final iron. Due to this Al enrichment, the growth of iron crystals during the reduction process is minimised resulting Fe particles with improved coercivity and squareness. Nevertheless, the coating procedure seems to be more effective giving rise to the iron particles with the largest coercivity, probably due to a better preservation of the acicular morphology in this case.

Keywords: Aluminium, Goethite, Iron nanoparticles, Magnetic properties

Nanopartículas aciculares de hierro protegidas frente a la sinterización con óxido de aluminio

Se han obtenido nanopartículas aciculares de hierro por reducción térmica con hidrógeno de un precursor acicular de goetita que fue protegido frente a la sinterización por la adición de cationes Al mediante dopado durante su síntesis o por recubrimiento posterior, estudiándose la relación entre la microestructura y las propiedades magnéticas de las partículas finales de α-Fe con objeto de evaluar la eficacia de ambos métodos de protección. Los precursores uniformes de goetita y de goetita dopada con Al se prepararon por oxidación con aire de disoluciones de $FeSO_4$ o de $FeSO_4$ y $Al(NO_3)_3$, previamente precipitadas por la adición de Na_2CO_3, mientras que el recubrimiento con óxido de aluminio sobre las partículas de goetita fue llevado a cabo por un procedimiento de heterocoagulación. En ambos métodos de protección, los cationes aluminio estaban principalmente concentrados en las capas más externas de las partículas, tanto de los precursores de goetita como del hierro. Debido a este enriquecimiento en Al, se minimiza el crecimiento de los cristales de hierro durante el proceso de reducción resultando partículas de Fe con mayores valores de coercitividad y de cuadratura de la curva de histéresis. No obstante, las partículas de hierro protegidas mediante recubrimiento presentaban valores de coercitividad ligeramente mayores, probablemente debido a la mejor conservación de la morfología acicular en este caso.

Palabras clave: Aluminio, Goetita, Nanopartículas de hierro, Propiedades magnéticas

1. INTRODUCTION

Commercial metal particles for recording media are usually produced starting from different iron hydroxide or oxide precursors which, through dehydroxylation to hematite ($α$-Fe_2O_3) when required, are converted to $α$-Fe metal particles after thermal reduction. The products are subjected also to a passivation treatment forming a surface layer of iron oxide around the particle in order to prevent further oxidation of the metal core (1,2). For this application acicular nanoparticles of $α$-Fe are required due to the low value of the demagnetization field along the major axis, which drives to higher coercitivy values (3). For the preparation of these iron particles, goethite that growths as elongated particles following its crystallographic habit, is usually used as precursor, which must be transformed to iron preserving the acicular morphology. In general, reduction of these precursors destroys the acicular morphology, which has undesirable effect on the magnetic properties of the final ferromagnetic metal cores. For this reason, the addition of preventing sintering agents, such as Al, B, Si, P and Sn, to the starting goethite particles has been suggested to preserve their acicular morphology during the formation of the metal particles (4).

Recently, we have prepared acicular iron nanoparticles by reduction of uniform goethite particles obtained in the presence of carbonate ions (5). Moreover, it was also shown that the use of an Al-doped precursor resulted in an important improvement of the magnetic properties of the final metal particles (6). In this work, Al cations have been incorporated to the undoped precursor particles by coating after their synthesis through a heterocoagulation process, and the relationship between the microstructural features and the magnetic properties of the final $α$-Fe particles was studied and compared to those of the Al-doped system, in order to evaluate the efficiency of both protecting methods to prevent sintering.

2. EXPERIMENTAL PROCEDURE

2.1. Precursor preparation

For the preparation of the acicular goethite, a 0.15 mol dm^{-3} Fe(II) sulphate ($FeSO_4 \cdot 7H_2O$, Aldrich, 99%) aqueous solution was precipitated by the addition of 0.225 mol dm^{-3} sodium carbonate (Na_2CO_3, Aldrich,

99.5%) and the resulting dispersion was then oxidized at constant temperature (40ºC) by bubbling air at constant flow rate (2 dm^{3}min^{-1}) for 6 hours, following the method described earlier (5). The precursor synthesized by this method is named as G.

Al(III)-doped goethite particles were obtained by adding the desired amount of Al(III) nitrate (Al(NO$_3$)$_3$·9H$_2$O, Fluka, 99%) to the Fe(III) sulphate aqueous solution before the addition of sodium carbonate (6). The sample synthesized by this method is named as G$_{Al}$.

Undoped goethite particles (sample G), were coated with aluminium hydrous oxide layers. The coating process involved first the dissolution of the desired amount of Al(NO$_3$)$_3$ in 150 ml of double distilled water and the addition of a 10% NaOH aqueous solution to reach a pH of 12.5. The goethite particles (150 mg) were homogeneously suspended in this solution using an ultrasonic bath and, finally, the pH was lowered to 8.5 by the slow addition of HNO$_3$ (0.5 mol dm^{-3}) into the slurry (7). The sample synthesized by this method is named as G$_{(Al)}$.

All precipitates were centrifuged and washed several times with deionised water for purification. Finally, the powdered solids were collected by filtration and dried at 50ºC before analyses.

2.2. Thermal Reduction

To obtain the final metal particles, the goethite samples (~60 mg) were dehydrated by heating in air for 4 h yielding hematite which was then reduced, at constant temperature in a hydrogen (99.9999%) stream (flow rate = 20 l h^{-1}) for 4 h. Dehydroxylation and reduction temperatures were optimised in each case to get complete reduction, as well as to minimise particle sintering. After reduction, the samples were cooled down to room temperature, under the hydrogen atmosphere, and, finally, passivated by exposing them to alcohol vapours for 1 hour, which were generated by bubbling N$_2$ gas (99.999%) at constant flow rate (40 dm^{3}h^{-1}) into a flask containing pure ethanol (99.8%). Metal samples prepared after reduction of G, G$_{Al}$ and G$_{(Al)}$ powders are named as Fe, Fe$_{Al}$ and Fe$_{(Al)}$ respectively.

2.3. Characterisation Techniques

Transmission Electron Microscopy (TEM, Philips 200 CM) was used to examine the morphology of the particles. The particle size distribution of the powders was evaluated from the electron micrographs by counting around one hundred particles. From these data, the degree of polydispersity, defined as the standard deviation (SD)/mean size (8), was evaluated. The mean and the SD values associated with the axial ratio (L/W) were evaluated from the L/W ratios obtained for each particle.

Phase identification was carried out by X-ray diffraction (XRD) in a Siemens D501 apparatus using CuKα radiation and a diffracted beam graphite monochromator. An estimation of the crystallite size was determined from the full width at half maximum of the XRD selected reflection by using the Scherrer equation (9). Differential thermal (DTA) and thermogravimetric analyses (TGA) (Seiko, EXSTAR 6000) were carried out in air at a heating rate of 10ºC min^{-1}.

The quantitative composition of the samples in terms of the Al and Fe contents was determined by X-ray fluorescence (XRF, Siemens SRS 3000). Energy dispersive X-ray analysis (EDX, Philips DX4), installed in the TEM microscope, was also used to gain information on the homogeneity of the particles composition. The variation of the aluminium and iron concentrations in the particle outer layers during the transformation from goethite to hematite, and finally to iron was obtained from the X-Ray Photoelectron spectra (XPS), recorded in a

VG Escalab 220 using the MgKα excitation source. Calibration of the binding energy scale of the spectra was done at the C1s peak of the surface carbon contamination taken at 284.6 eV. Atomic percentages of the elements were calculated from the peaks areas after background subtraction (Shirley background). The areas were referred to the sensitivity factors of the elements as supplied by the instrument manufactures.

Temperature programmed reduction (TPR) experiments were performed in a conventional apparatus connected to a computer for data storing and processing, using a thermal conductivity detector, (TCD) calibrated using different amounts of CuO, as previously described (10). The reactive gas (5% H$_2$ in Ar, flow rate = 50 cm^3 min^{-1}) was passed through 5 mg of sample, which was heated up to 600ºC at a constant heating rate of 5ºC min^{-1}.

Magnetic characterization of the samples was carried out in a vibrating sample magnetometer (MLVSM9 MagLab 9 T, Oxford Instrument). Magnetization curves were recorded at room temperature by first saturating the sample in a field of 3 T; then, the saturation magnetization (M$_s$), the squareness (M$_r$/M$_s$, where M$_r$ is the remanent magnetization) and the coercivity (H$_c$) were determined for each sample. The M$_s$ values were evaluated by extrapolating to infinite field the experimental results obtained in the high field range where the magnetization linearly increases with 1/H.

3. RESULTS AND DISCUSSION

3.1. Precursors Preparation

Uniform goethite particles (Fig. 1) of 118 nm in length with axial ratio of 5 (Table I) were obtained following the method described in experimental section (Sample G). Under the same conditions, the addition of Al cations up to a Al/Fe+Al mole ratio = 5% (Sample G$_{Al}$) yielded single phase goethite particles (Fig. 1) with an aluminium content similar to that initially added (Table I). The presence of aluminium yielded shorter particles (62 nm in length) that the undoped ones, keeping similar particle width, and broader size distribution (Table I). These morphological changes have been attributed to isomorphous substitution of Al^{3+} for Fe^{3+} in the goethite structure (11). It has been already reported that the Al cations were mainly concentrated in the particle outer layers in spite of being in the reaction medium from the beginning of the goethite preparation (6).

TABLE I.- Composition and morphological characteristics (length, width and axial ratio) observed for goethite precursors (the relative standard deviations are included in parenthesis).

Sample	Morphological Characteristics			Al/Fe+Al mole ratio		
	Length (nm)	Width (nm)	Axial Ratio	Nominal (%)	XRF (%)	XPS (%)
G	118 (20)	24 (29)	5 (30)	-	-	-
G$_{Al}$	62 (28)	23 (33)	3 (33)	5	5	17
G$_{(Al)}$	118 (20)	24 (29)	5 (30)	5	5	80

Goethite particles were also coated with uniform layers of an aluminium hydrous oxide using an Al/Al+Fe ratio similar to that of the doped sample (Al/Fe+Al mole ratio = 5%). As it can be seen in the TEM images (Fig. 1), only acicular particles were present in the coated sample, suggesting that all precipitated aluminium hydrous oxide was deposited on the surface of goethite particles. The amount of aluminium incorporated on the goethite surface was confirmed to be similar to that initially added (Table I) and EDX analyses confirmed the presence of Al in all analysed particles. Finally, XPS spectroscopy
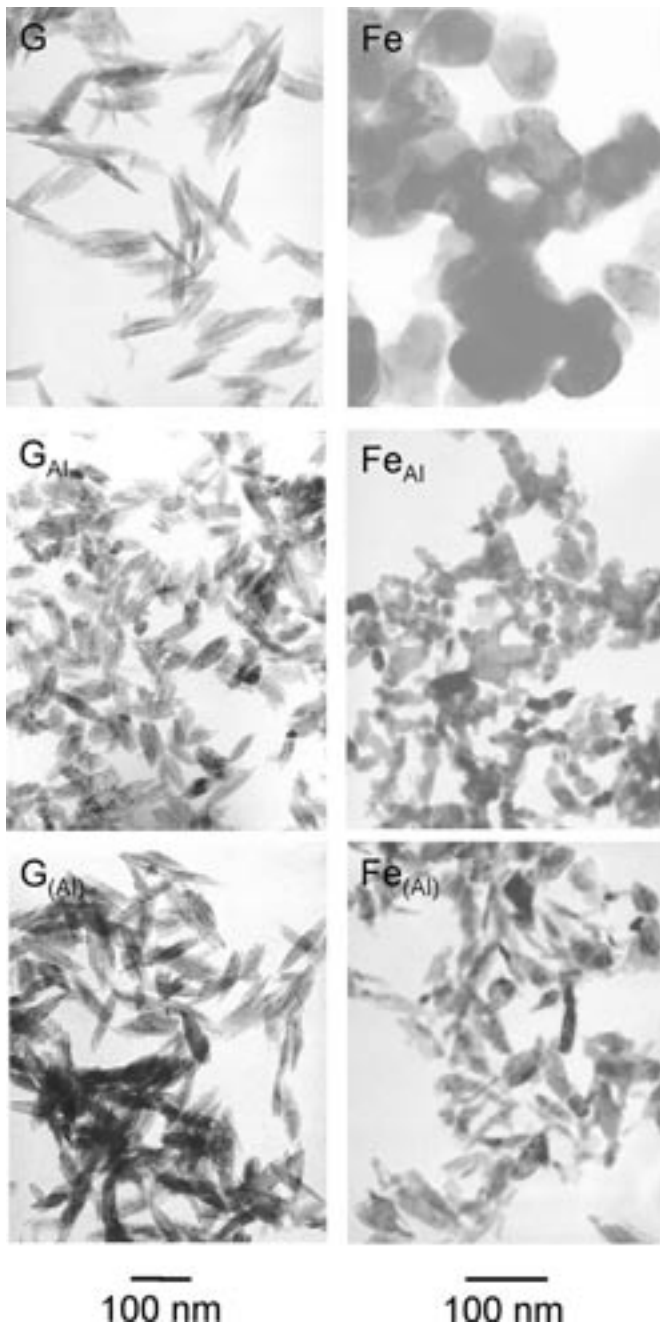
Bol. Soc. Esp. Ceram. V., 43 [4] 796-800 (2004)

797

Figure 1.- TEM images for goethite (G), Al(III)-doped goethite (G_{Al}) and Al(III)-coated goethite ($G_{(Al)}$) samples and the corresponding iron particles obtained after reduction (Fe, Fe_{Al} and $Fe_{(Al)}$ samples).

Figure 2.-TG and DTA analyses for goethite (G) and Al-coated goethite ($G_{(Al)}$) samples.

Figure 3.- TPR profiles for the hematite samples obtained by heating at 300ºC the undoped (G), Al(III)-doped (G_{Al}) and Al(III)-coated ($G_{(Al)}$) goethite precursors.

showed a more important enrichment of Al (Al/Fe+Al mole ratio = 80%) in the particle outer layers in comparison with the Al(III)-doped goethite sample (17% mole), which is as it should be expected from the coating procedure (Table I).

A slight increase in the thermal stability of the goethites prepared in the presence of aluminium with respect to the Al-free goethites was detected by TG and DTA analyses as illustrated for the coated sample (Fig. 2). As observed, the strong endothermic peak, which is due to the conversion of goethite to hematite, was displaced from 250ºC for sample G to 257ºC for sample $G_{(Al)}$. This higher temperature of dehydroxylation can be attributed to the enrichment of aluminium in the particle outer layers since it could hamper the transport of the released water (12).
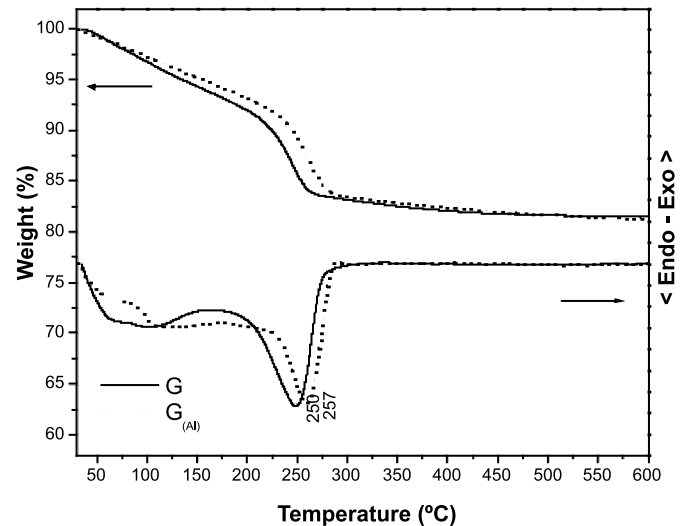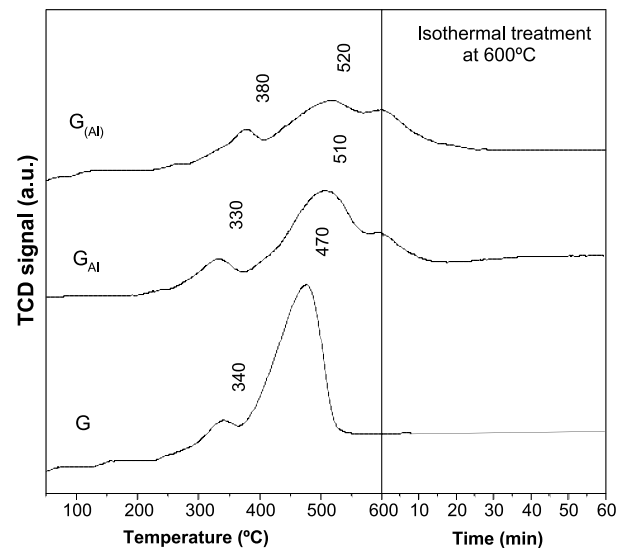
3.2. Iron Metallic Particles

3.2.1. THERMAL REDUCTION OF SAMPLES

The goethite particles were transformed to metallic iron in two steps, aiming to reduce internal porosity and avoid further alterations of the particle morphology (1). First, the goethite particles were transformed to hematite by heating up to maximum temperature so that the particle morphology remained unaffected in the unprotected sample (300ºC). The so-obtained hematite samples were then reduced to metal iron, for which the reduction temperature was also optimized in order to minimize the possible particle morphology alteration during this treatment. For this purpose, temperature programmed reduction (TPR) experiments were carried out. The TPR profiles of the undoped goethite samples (Fig. 3) clearly showed that the reduction process took place under the non-isothermal conditions, from 250ºC to 550ºC in two well-resolved reduction steps. The hydrogen uptakes obtained

798

Bol. Soc. Esp. Ceram. V., 43 [4] 796-800 (2004)

by numerical integration of the peaks areas indicated that the first step (~340 °C) was due to the transformation of hematite to magnetite (Fe_3O_4), whereas the second one (~470 °C), was due to the magnetite-metal iron reduction. Finally, the TPR profiles also suggested that the presence of aluminium cations in the hematite precursors (either in the doped or coated samples) retards the reduction process (Fig. 3). In fact, an isothermal treatment at 600 °C was further required in both cases to complete the reduction reaction (Fig. 3). It has been reported that the reduction rate to iron is mostly controlled by the removal of water (13). Therefore, it seems that the presence of Al ions at the particle surface hamper the transport of water, needing higher reduction temperatures for its total release. Fig. 3 also shows that the only appreciable difference in the reduction behaviour between the doped (G_{Al}) and coated ($G_{(Al)}$) samples is that the first reduction step (Fe_3O_4 formation) takes place at lower temperature for the former.

In view of these results, the hematite samples were reduced under the isothermal conditions described in the experimental section, at increasing temperatures starting from 250°C to find the minimum temperature required to complete reduction which, as expected, was higher for both Al-doped and Al-coated samples (400°C) than that for the unprotected one (325°C).

X-ray diffraction patterns for all the samples reduced at the above temperatures are shown in Fig. 4. Samples Fe and $Fe_{(Al)}$ display a similar pattern with diffraction peaks only due to α-Fe. However, in addition to the main diffraction peaks due to α-Fe, sample Fe_{Al} shows a broad and very weak peak around 35° (2θ), which could be due to the presence of small crystallites of an iron oxide with a spinel structure (14). This oxide could be formed during the passivation process carried out to stabilize the particles. The higher amount of oxide in this sample could be due to its smaller particle size (Fig. 1), and therefore higher surface area. The crystal size measured from the (100) reflection of iron was observed to decrease for the Al(III)-protected metal samples (Table II). These data suggest that the presence of aluminium minimises the growth of iron crystals during the thermal reduction process, and clearly evidence its role in preventing sintering.

TABLE II.- MAGNETIC PROPERTIES (M_s = SATURATION MAGNETIZATION, H_c = COERCIVITY, M_r = REMANENT MAGNETIZATION AND M_r/M_s = SQUARENESS) AND CRYSTAL SIZE OBTAINED FOR IRON (Fe), AL-DOPED IRON (Fe_{Al}) AND AL-COATED IRON ($Fe_{(Al)}$) SAMPLES.

Sample	Reduction Temperature (°C)	Crystal Size (nm)	H_c (Oe)	M_s (emu/g)	M_r/M_s
Fe	325	200	110	205	0.05
Fe_{Al}	400	30	920	125	0.5
$Fe_{(Al)}$	400	35	1050	120	0.4

Metal particles obtained from the goethite samples show different morphological characteristics. Thus, in the absence of aluminium (sample Fe), the particles sintered during the reduction process losing the elongated shape (Fig. 1), which is in accordance with the higher crystal size measured for this sample (Table II). However, this process took place in a lesser extension for the Fe_{Al} and $Fe_{(Al)}$ samples, in which more elongated particles remained, especially in the case of sample $Fe_{(Al)}$ (Fig. 1). It is clear that in this sample, the aluminium oxide coating is the responsible for preventing sintering. For a better understanding of the behaviour observed for sample Fe_{Al}, the variation of the Al(Fe+Al) ratio at the particle outer layers during the transformation from goethite to hematite and then, to metal iron, was followed by XPS finding that the molar percentage of Al(III) increases from 18% (goethite) to 36 % (iron) (Fig. 5). Thus, there is a further clear Al enrichment in the particle outer layers during reduction, which explains the absence of a significant sintering observed for
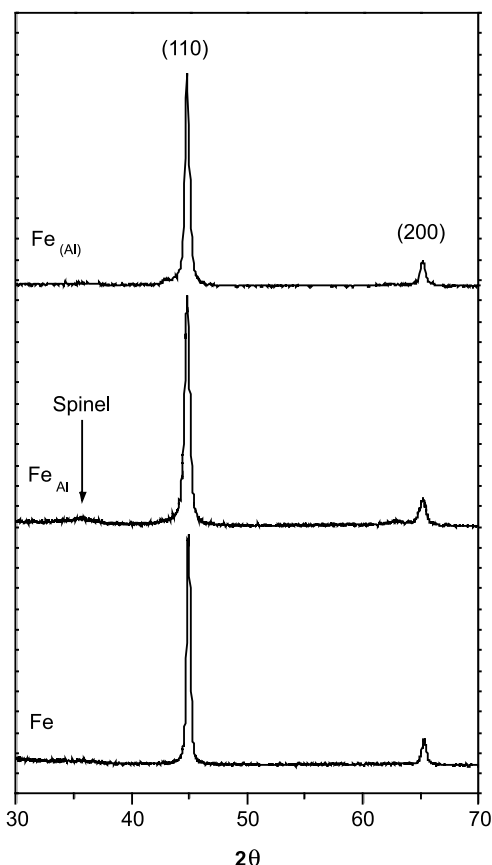

Figure 4.- X-Ray diffraction patterns for samples Fe, Fe_{Al} and $Fe_{(Al)}$ metal samples.
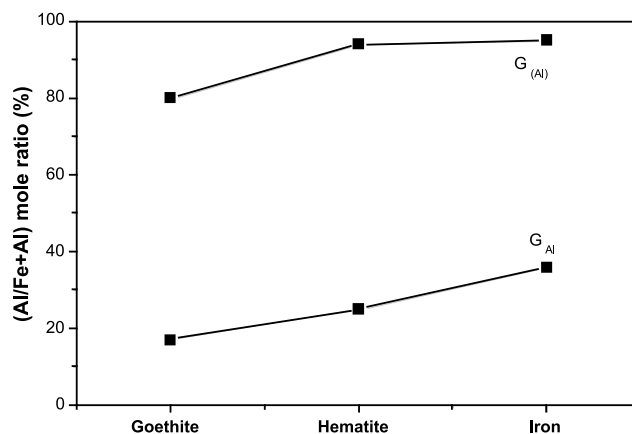

Figure 5.- Variation of the aluminium concentration in the particle outer layers obtained from XPS spectra during the transformation from goethite to hematite and finally to metal iron for Al-doped goethite (G_{Al}) and Al-coated goethite ($G_{(Al)}$) samples.

this sample, in which these cations were introduced into the goethite precursor during its synthesis (6). This enrichment was higher for the Al(III)-coated particles (from 80% for goethite, to 95% for iron) (Fig. 5), which would explain the better acicular morphology observed for this sample (Fig. 1). It should be noted that the position of the $Fe2p_{3/2}$ peak observed in the XPS spectra (710.1 eV) (data not shown) was consistent with the presence of the above mentioned oxidized iron in the particle outer layers, which seems to be consist of a ferrimagnetic oxide similar to Al(III)-doped maghemite, as it has been suggested from Mössbauer studies carried out on the Fe_{Al} sample (6).

Bol. Soc. Esp. Ceram. V., 43 [4] 796-800 (2004)

799

3.2.2. MAGNETIC PROPERTIES OF IRON NANOPARTICLES

The magnetic parameters obtained from the magnetization curves represented in Fig. 6 are summarized in Table II. All values obtained for saturation magnetization (M_s) are lower than it is expected for bulk Fe (~220 emu/g) (15), due to the presence of iron oxide on the particle surface resulting from passivation (6). The largest M_s values obtained for the Fe sample when compared with the Al(III)-protected samples, can be explained by the higher crystal size of the former, which therefore involved a lower relative oxide amount in the passivation layer, and obviously by the presence of non-magnetic aluminium oxide on the particle surface in the protected samples (16).

It should be noted that the increase in the M_r/M_s (Squareness) values observed for the Al(III)-protected particles (from 0.05 for sample Fe to 0.4 and 0.5 for samples $Fe_{(Al)}$ and Fe_{Al}, respectively) suggests a change from a multidomain behaviour for the Al(III)-free samples to a monodomain behaviour for Al(III)-protected samples, according to the decrease in the Fe crystal size observed by X-ray diffraction from 200 to 30-35 nm (Table II) (17).

The incorporation of aluminium cations to the precursor particles either by doping or coating, also had positive effects on the coercivity (H_c) of the final metal samples (Table II). Thus, the coercivity increases from 110 Oe for the unprotected sample (Fe) to 920 and 1050 for samples Fe_{Al} and $Fe_{(Al)}$, respectively. This increase seems to be due to the minimisation of sintering, preserving the acicular morphology of the particles, since it is well known the main factor that contributes to the increase of coercivity in these materials is shape anisotropy. Slightly higher H_c value (1050 Oe), was found for the sample protected by coating ($Fe_{(Al)}$ sample), indicating that this protecting procedure is slightly more effective to produce iron metal particles with better magnetic properties.

4. CONCLUSIONS

Both protecting methods of goethite particles, Al(III)-doping and Al(III)-coating, drive to an Al-enrichment on the goethite particles surface, which is increased during the transformation to iron. This enrichment minimises the growth of iron crystals and better preserves the acicular shape in the final iron particles, which has a favourable effect on the squareness and coercivity of both metal samples. This behaviour indicates the effectiveness of both method to protect the acicular iron nanoparticles against sintering and therefore to obtain materials with improved magnetic properties. Nevertheless, the coating procedure seems to be slightly more effective giving rise to the iron particles with the largest coercivity.
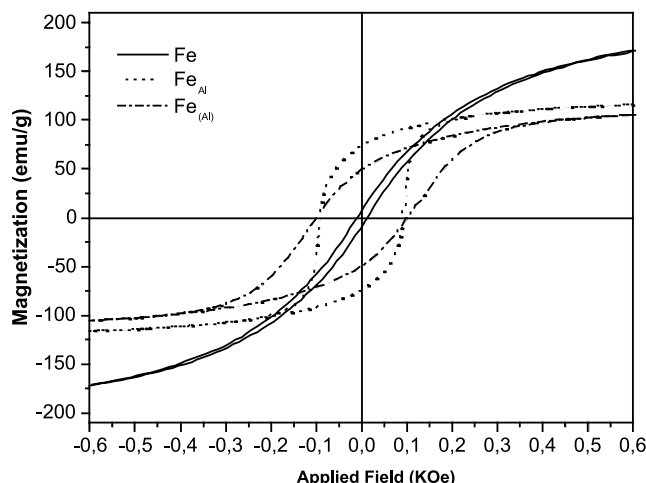
Figure 6.- Magnetization curves at room temperature for samples Fe, Fe_{Al} and $Fe_{(Al)}$ metal particles obtained by thermal reduction of the goethite precursors.

REFERENCES

1. S. Hisano and K. Saito, "Research and development of metal powder for magnetic recording", J. Magn. Magn. Mater. **190**, 371-381 (1998).
2. M.P. Morales, S.A. Walton, L.S. Prichard, C.J. Serna, D.P.E. Dickson and K. O´Grady, "Characterisation of advanced metal particle recording media pigments", J. Magn. Magn. Mater. **190**, 357-370 (1998).
3. R.J. Veitch, A. Ilmer, W. Lenz and V. Richter, "MP technology for a new generation of magnetic tapes", J. Magn. Magn. Mater. **193**, 279-283 (1999).
4. M.P. Sharrock, "Recent advances in metal particulate recording media: Toward the ultimate particle", IEEE Trans. Magn. **36**, 2420-2425 (2000).
5. R. Pozas, M. Ocaña, M.P. Morales and C.J. Serna, "Uniform nanosized goethite particles obtained by aerial oxidation in the $FeSO_4$-Na_2CO_3 system", J. Colloid Interf. Sci. **254**, 87-94 (2002).
6. N.O. Nuñez, R. Pozas, M.P. Morales, P. Tartaj, P. Bonville, A.R. González-Elipe, A. Caballero, M. Ocaña and C.J. Serna, "Acicular metallic particles obtained from Al-doped goethite precursors", Chem. Mater., **15**, 951-957 (2003).
7. S. Hisano, K. Saito, S. Aizawa, K. Sano, K. Matsumoto and K. Murata, Dowa Mining Co., Ltd., Tokyo, Japan, "Ferromagnetic metal powder". US Patent No, 5591535, (1997).
8. R. Hunter, "Foundations of Colloid Science", Clarendon Press: Oxford, UK, (1987), p.127.
9. L. V. Azároff, "Elements of X-ray Crystallography", McGraw-Hill: New York, USA, (1968), p.549.
10. P. Malet, G. Munuera and A. Caballero, "Effect of chlorine in the formation of PtRe alloys in PtRe/Al_2O_3 catalysts", J. Catal., **115**, 567 (1989).
11. D.G. Schulze and U. Schwertmann, "The influence of aluminium on iron oxides: X. Properties of Al-substituted goethites", Clay Miner. **19**, 521-539 (1984).
12. K. Jonás and K. Solymár, "Preparation, X-ray, derivatographic and infrared study of aluminium-substituted goethites", Acta Chim. Acad. Sci. Hung., **66**, 383 (1970).
13. A.A. Van der Giessen and C.J. Klomp, "The preparation of iron powders consisting of submicroscopic elongated particles by pseudomorphic reduction of iron oxides", IEEE Trans. Magn., **5**, 317-320 (1969).
14. JCPDF file No 39.1346.
15. B.D. Cullity, "Introduction to Magnetic Materials", Addison-Wesley, CA, USA, (1972).
16. C.H. Lin, T.S. Chin, P.C. Kuo, S.C. Chen and C.S. Shih, "Preparation and magnetic properties of Al_2O_3-coated acicular α-Fe particles", Mater. Chem. Phys. **44**, 90-94 (1996).
17. T. Sueyoshi, K. Tashita, S. Hirai, M. Kishimoto, Y. Hayashi and M. Amemiya, "Effect of heat treatment on magnetic properties and morphology of iron particles", J. Appl. Phys. **53**, 2570-2572 (1982).

◆ ◆ ◆